Ph. Geyer, J. M. Proix,† Ph. Schoenberger,‡ and S. Taheri‡*

A Three-dimensional Elastoplastic Cyclic Constitutive Law with a Semi-discrete Variable and a Ratchetting Stress

REFERENCE Geyer, Ph., Proix, J. M., Schoenberger, Ph., and Taheri, S., **A three-dimensional elasto-plastic cyclic constitutive law with a semi-discrete variable and a ratchetting stress,** *Multiaxial Fatigue and Design*, ESIS 21, (Edited by A. Pineau, G. Cailletaud, and T. C. Lindley) 1996, Mechanical Engineering Publications, London, pp. 139–152.

ABSTRACT The study of cyclic elastoplastic constitutive laws has focused on nonproportional loadings, but for uniaxial loadings some problems remain, as for example the ability for a law to describe simultaneously ratchetting (constant increment of strain) in nonsymmetrical load-controlled test, elastic and plastic shakedown in symmetrical and nonsymmetrical cases. Previously, we have proposed a law with a discrete memory variable, the plastic strain at the last unloading, and a ratchetting stress which, in addition to earlier phenomena, describes the cyclic hardening in a push-pull test, and the cyclic softening after overloading. On the other hand the choice of all macroscopic variables is justified by a microscopic analysis. A modified law was proposed to take into account the dependence of cyclic stress–strain curves on the history of loading. The extension to three-dimensional situations of this law was proposed. The discrete nature of the memory leads to discontinuity problems for some loading paths, a modification is then proposed which uses a differential evolution law. For large enough uniaxial cycles, the uniaxial law is nevertheless recovered. An incremental form of the implicit evolution problem is given, and we describe the implementation of this model in the *Code Aster*© a thermomechanical structural software using FEM, developed at Electricité de France. In this paper we briefly explain the model and we present some comparisons between experiments and numerical results, for nonproportional strain-controlled tests (circular, square, stair loading), and constant-tension cyclic torsion tests, on a 316 stainless steel, using uniaxial identification.

1 The Microstructure under Cyclic Loading

When the cross-slipping of dislocations is possible for a metal – easy cross-slip for pure Al and pure Cu, difficult cross-slip for a 316 stainless steel – the microstructure is characterized at low cyclic amplitude by permanent slip bands and at higher amplitude by cell structure, whose mean size decreases with an increasing amplitude of loading. But when the amplitude of loading decreases, the cell structure is stable at room temperature. The cell structure seems also to be detected for a monotonic loading. As before the cell size decreases with increasing strain.

*Direction des Etudes et Recherches, Les Renardières, 77250 Moret sur Loing, Electricité de France.
†SEPTEN, 12–14 Avenue Dutrievoz, 69628, Villeurbanne, Electricité de France.
‡Direction des Etudes et Recherches, 1 Avenue Général de Gaulle, 92141, Clamart, Electricité de France.

We suppose that the mean cell size is defined by the maximal stress supported by the material in its history. The asymptotic form of the curves showing mean cell size as a function of the amplitude of loading suggests to us to suppose the existence of a minimal cell size depending only on the material and not on the loading. During cycling, dislocations pile up on the obstacles (walls), and the steady-state is obtained when the numbers of dislocations created and annihilated are equal. The plastic strain is then created by dislocations which sweep away the cell volume or PSB, and then are annihilated by dislocations of opposite sign. If the loading amplitude is increased after obtaining steady-state at a first level, smaller cells will be obtained. That means that new obstacles are created, on which dislocations have to pile up again. More than one cycle is needed to get a new stabilized state. This is macroscopically illustrated by a push-pull test, and characterizes the interaction between dislocation density and cell size.

Different experiments show that, at room temperature, ratchetting is practically obtained at a nearly constant maximal stress, independently of the amplitude of loading (6). This suggests the use of a cyclic ultimate stress S – the ratcheting stress – which we relate to a minimal cell size. The idea of a threshold for ratchetting has been also used by other authors (7).

This paper builds on earlier published work (1–5).

2 Definition of Macroscopic Variables through Microstructure

We define now more precisely the macroscopic variables in relation to the microscopic analysis.

- ε^p, usual plastic part of the strain, related to the gliding of dislocations.
- σ_p, maximal past absolute value of stress supported by the material in its history, related to the actual cell mean size: this variable is used in $S - \sigma_p$, where S is the ratchetting stress.
- ε_n^p, plastic deformation at the last unloading point. Here, the significant variable is the difference $\varepsilon^p - \varepsilon_n^p$, on steady-state. It measures the amplitude of plastic strain, which may be related to sweeping of cell volume by the active dislocations.
- λ, cumulated plastic strain, related to the density of dislocations. In order to take into account the interaction between cell size and disloction density, we use instead the variable.

$$\lambda\left(1 - \frac{\sigma_p}{S}\right)$$

3 Uniaxial Constitutive Law

3.1 *Natural introduction of* ε_n^p

In the case of ratchetting, after a few cycles the tension and compression curves

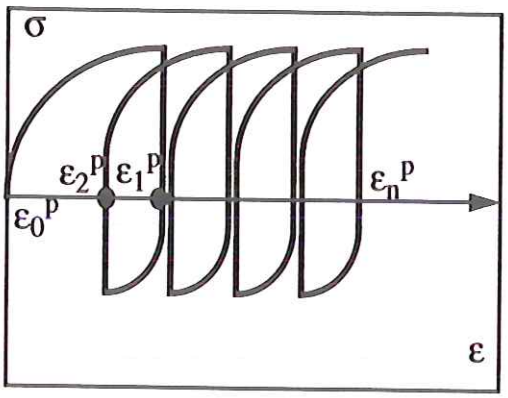

Fig 1 Definition of ε_n^p.

are translated at each cycle of a constant value, see Fig. 1. Using two functions g and h, we have

$$\sigma_t = h(\varepsilon^p - \varepsilon_{2n}^p) \quad \text{and} \quad \sigma_c = g(\varepsilon^p - \varepsilon_{2n+1}^p)$$

with h', g', $g'' > 0$ and $h'' < 0$, where ε_{2n}^p (resp. ε_{2n+1}^p) is the plastic strain at the last unloading on the compression (resp. tension) curve. These variables have been used in a different way (**8**). We suppose that there is no ratcheting phenomena for a symmetric loading; for $\sigma_{min} = -\sigma_{max}$, we obtain plastic or elastic shakedown. It is possible, using two functions A and B, to show that the general form of tension and compression curves in the ratchetting state are as follows

$$\sigma_t = (\varepsilon^p - \varepsilon_{2n}^p)A(|\varepsilon^p - \varepsilon_{2n}^p|) + B(|\varepsilon^p - \varepsilon_{2n}^p|)$$

$$\sigma_c = (\varepsilon^p - \varepsilon_{2n}^p)A(|\varepsilon^p - \varepsilon_{2n+1}^p|) - B(|\varepsilon^p - \varepsilon_{2n+1}^p|)$$

We studied the case for $A = 0$ (**1**). It has been shown in this case that the law may describe the following phenomena

- ratchetting in a non-symmetrical load-controlled test,
- elastic and plastic shakedown in symmetrical and non symmetrical test,
- cyclic hardening in a push-pull test,
- cyclic softening after overloading and also the dependence of cyclic-stress-strain-curve on the history of loading.

However the difficulty in this case comes from the bad representation of the cyclic stress–strain curve obtained after prehardening, and also from the linear relation between mean stress and mean strain.

The case for $A = K$, with K a non-zero constant, is described in (**2**), and here. However a better result may probably be obtained by a nonlinear function.

$$\sigma_t = K(\varepsilon^p - \varepsilon^p_{2n}) + B(|\varepsilon^p - \varepsilon^p_{2n}|)$$

$$\sigma_c = K(\varepsilon^p - \varepsilon^p_{2n+1}) - B(|\varepsilon^p - \varepsilon^p_{2n+1}|)$$

This remembers the yield function with combined kinematic isotropic hardening in three-dimensional situations.

$$\sqrt{\left\{\frac{3}{2}(s_{ij} - x_{ij})(s_{ij} - x_{ij})\right\}} - R = 0$$

which gives under uniaxial loading

$$\sigma_t = \frac{3}{2} X_{11} + R \quad \text{in tension}$$

$$\sigma_c = \frac{3}{2} X_{11} - R \quad \text{in compression}$$

3.2 *Introduction of a ratchetting stress S*

We suppose that in the uniaxial case ratchetting (constant increment of strain) is obtained when the maximal stress in absolute value σ_p reaches the value S (2). But for the stresses smaller than this value we have elastic or plastic shakedown. The simplest way to obtain this result is to transform the expression

$$K(\varepsilon^p - \varepsilon^p_{2n}) \quad \text{into} \quad K(S\varepsilon^p - \sigma_p \varepsilon^p_{2n})$$

The expression of tension and compression curves in the case of plastic shakedown are

$$\sigma_t = K(S\varepsilon^p - \sigma_p \varepsilon^p_{2n}) + B(|\varepsilon^p - \varepsilon^p_{2n}|)$$

$$\sigma_c = K(S\varepsilon^p - \sigma_p \varepsilon^p_{2n+1}) - B(|\varepsilon^p - \varepsilon^p_{2n+1}|)$$

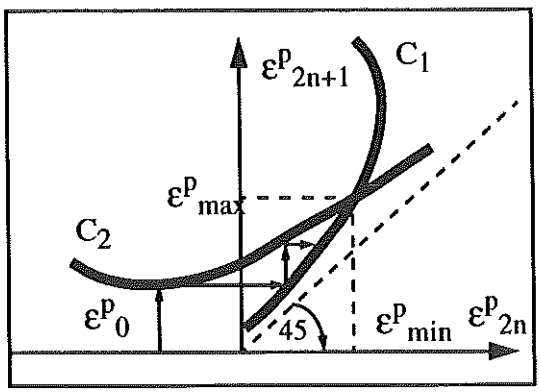

Fig 2 Plastic shakedown.

It is then possible to describe schematically the onset of ratchetting and plastic shakedown. In fact, the above two relations constitute a recurrent process. We get two curves with $X = \varepsilon^{p}_{2n}$; $Y = \varepsilon^{p}_{2n}$

$$\text{Curve C1: } K(SY - \sigma_p X) + B(|Y - X|) - \sigma_{max} = 0$$

$$\text{Curve C2: } K(SX - \sigma_p Y) - B(|Y - X|) - \sigma_{min} = 0$$

For $S > \sigma_p$, C1 and C2 are two intersecting curves and with an initial state of strain ε^{p}_{0}, plastic or elastic shakedown is obtained as shown in Fig. 2. For $S = \sigma_p$, C1 and C2 are two parallel lines, so that ratchetting is present. However if $\sigma_{max} = -\sigma_{min}$ the two lines are superposed and plastic or elastic shakedown is obtained.

3.3 *Introduction of the cumulated plastic strain* λ

The introduction of this variable allows us to describe hardening or softening for strain-controlled tests. However, once steady-state is obtained in a strain-controlled test, for a greater strain amplitude the steady-state will be obtained in one cycle. This difficulty will be erased if we use the parameter $\lambda(1 - \sigma_p/S)$ instead of λ. Finally as a simple choice using two functions K and f(2), we may take:

$$\sigma_t = K\left(\lambda\left(1 - \frac{\sigma_p}{S}\right)\right)(S\varepsilon^p - \sigma_p \varepsilon^p_{2n}) + f\left(\lambda\left(1 - \frac{\sigma_p}{S}\right)\right)B(|\varepsilon^p - \varepsilon^p_{2n}|)$$

$$\left[\sigma_c = K\left(\lambda\left(1 - \frac{\sigma_p}{S}\right)\right)(s\varepsilon^p - \sigma_p \varepsilon^p_{2n+1}) - f\left(\lambda\left(1 - \frac{\sigma_p}{s}\right)\right)B(|\varepsilon^p - \varepsilon^p_{2n+1}|)\right]$$

The resulting properties are as follows.

(1) The usual cyclic stress–strain curve for a symmetric loading is given by

$$y = \frac{(\frac{3}{2}K_\infty Sx + B(2x)}{1 - \frac{3}{2}K_\infty x} \text{ where } \begin{cases} y = \dfrac{\Delta\sigma}{2} & x = \dfrac{\Delta\varepsilon^p}{2} \\ x < \dfrac{2}{3K_\infty} & K_\infty = K(\lambda \to \infty) \end{cases}$$

If there is a large prehardening σ_p, the cyclic curve is given by:

$$y = \frac{3}{2}K_\infty(s + \sigma_p)x + B(2x)$$

(2) The relation between σ_{mean} and ε^p_{mean} is

$$\sigma_{mean} = \frac{3}{2}K_\infty(s - \sigma_p)\varepsilon^p_{mean}$$

This gives a possibility of a good stress relaxation for large prehardening, which seems to be the case for 316 stainless steel.

4 The Three-dimensional Law

The extension to three-dimensional situations of the previous uniaxial law begins with the choice of the variables themselves. For the sake of simplicity the deviatoric part of the tensors is chosen as usually done, to keep the initial form of the uniaxial law. The constitutive law is now simply described by an elastoplastic model where the yield function combines isotropic and kinematic hardening

$$F(\sigma, \varepsilon^p, \lambda, \sigma_p, \varepsilon_n^p) = |\sigma_D - x(\varepsilon^p, \lambda, \sigma_p, \varepsilon_n^p)| - R(\lambda, \sigma_p, |\varepsilon^p - \varepsilon_n^p|)$$

The usual normality and consistency relations are used for the remaining variables ε_p and λ (3). But a difficulty arises from extension of the definitions and evolution equations of the memory variables σ_p and ε_n^p. As a matter of fact, the uniaxial loading histories are very poor: there is no tangent loading; cycling is only defined by two extreme values etc. Intrinsic definitions and more precise evolution laws are needed in the three-dimensional case. The variable σ_p is defined as the maximal past deviatoric norm of the stress experienced by the material – the norm is denoted by $|\sigma_D|$

$$\sigma_p(t) = \operatorname*{Max}_{u \in [0,t]} |\sigma_D(u)|$$

Note that σ_p may keep its initial value σ_p^0 during the loading history. We can rewrite this definition as a new yield function G in the deviatoric stress space

$$G = |\sigma_D| - \sigma_p$$

leading to the evolution equation for $\dot{\sigma}_p$ (H is the Heaviside function)

$$\dot{\sigma}_p = H(|\sigma_D| - \sigma_p) \frac{\sigma_D \dot{\sigma}}{|\sigma_D|}$$

Two problems arise from the definition of the evolution law of ε_n^p (3). The first one is that the material behaviour admits some undershooting of the monotonic stress–strain curve after an elastic unloading followed by reloading. However this is not always a disadvantage.

The second problem, more important from a physical point of view, is the requirement of continuity of the stress–strain curve with respect to very small unloadings. With full discrete memory, this requirement is generally not fulfilled: any unloading, even as small as possible, leads to a discontinuous evolution of the memory variable which induces in turn a discontinuity on the value of the yield function F. This last discontinuity can finally cause the violation of the yield condition ($F \leqslant 0$).

For three-dimensional loading paths, this problem is of primary importance because *micro-unloadings* can result from the change of direction of the loading

path in the stress space. To overcome this last difficulty, we modify the discrete evolution law for ε_n^p to semi-discrete one – the word semi-discrete is used because of the saturation of the memory ensuing from the definition of the evolution. Starting from the discrete model

$$\Delta\varepsilon_n^p = \varepsilon_n^{p+} - \varepsilon_n^{p-} = \varepsilon^p - \varepsilon_n^{p-} \quad \text{if} \quad F = 0 \quad \left(\dot{\sigma}\frac{\partial F}{\partial \sigma}\right) \leqslant 0$$

We introduce a scalar differential evolution together with a consistency condition ensuring the fulfilment of the yield condition.

$$\dot{\varepsilon}_n^p = \dot{\alpha}(\varepsilon^p - \varepsilon_n^p) \quad \text{if} \quad F = 0 \quad \left(\dot{\sigma}\frac{\partial F}{\partial \sigma}\right) \leqslant 0$$

$$\dot{\alpha} \geqslant 0 \qquad \dot{\alpha}F = 0 \qquad F \leqslant 0$$

α is a non-decreasing scalar parameter which may vary between 0 and 1 (**3**). It can be seen that, with appropriate generalized hardening conditions on the yield function F we have

- the yield condition ($F < 0$) is never violated;
- the continuity with respect to the chronology parameter is restored;
- the memory shows a *saturation effect*: if during the unloading, the value of ε_n^p reaches ε^p, then ε_n^p stays at this value and the unloading becomes purely elastic with no evolution of an internal variable;
- for uniaxial cycling loadings, the discrete memory is recovered between two successive unloadings, provided the cycle is large enough.

5 The Implicit Integration of the Three-dimensional Rates Equations

When $|\sigma_D|$ does not reach σ_p the present formulation reduces to a standard plasticity model.

Nonstandard flow rules are obtained when σ_p varies during loading (but normality for the plastic strain rate still remains valid). To write down extensively the proposed constitutive law, we present hereafter its implicit incremental form which will be used in computations. We denote by

- **e**, the 'mechanical state' (ε_p, λ, σ_p, ε_n^p);
- **A**, the elasticity tensor;
- **X**, the backstress tensor.

In order to integrate rate equations of the constitutive model over the increment Δt, we integrate the flow rule by the backward difference scheme

$$\Delta\varepsilon^p = \Delta\lambda\left(\frac{\partial F}{\partial \sigma}\right)_{t+\Delta t}$$

During plastic flow, the consistency condition is imposed at the end of increment

$$F_{t+\Delta t} = 0$$

The equations of elasticity are written at the end of the increment

$$\sigma_{t+\Delta t} = A_{t+\Delta t}\varepsilon^{e}_{t+\Delta t}$$

The rate of ε^{p}_{n} is integrated by the forward difference scheme in order to respect

$$[\varepsilon^{p}_{nt+\Delta t} = \varepsilon^{p}_{nt} + \Delta\varepsilon^{p}_{n} = \varepsilon^{p}_{t}]$$

At the end of increment, so we have

$$\Delta\varepsilon^{p}_{n} = \Delta\alpha(\varepsilon - \varepsilon^{p}_{n})_{t}$$

The value of the *pick function* G must also be zero at the end of the increment, when σ_{p} varies during loading

$$G_{t+\Delta t} = \sigma_{pt+\Delta t} - |X|_{t+\Delta t} - R_{t+\Delta t}$$

So, we can exhibit four types of increment for the model, by opposition with the two states, elastic and elastoplastic, of a standard plasticity model:

- A *purely elastic* increment (E), where only the variable σ is incremented.
- A *pseudo-elastic* increment (PE), where only ε^{p}_{n} and σ are actualized.

$$\begin{gathered}\Delta\varepsilon^{p}_{n} = \Delta\alpha(\varepsilon^{p} - \varepsilon^{p}_{n})_{t}\\ \sigma_{t+\Delta t} = A_{t+\Delta t}(\varepsilon_{t+\Delta t} - \varepsilon^{p}_{t})\\ F(\sigma_{t+\Delta t}, \varepsilon^{p}_{nt+\Delta t}, \varepsilon^{p}_{t}, \sigma_{pt}, \lambda_{t}) = 0\end{gathered} \tag{S1}$$

- An *elastoplastic* increment (EP), where σ, λ and ε^{p} are actualized.

$$\begin{gathered}\sigma_{t+\Delta t} = A_{t+\Delta t}\left(\varepsilon_{t+\Delta t} - \varepsilon^{p}_{t} - \Delta\lambda\left(\frac{\partial F}{\partial\sigma}\right)_{t+\Delta t}\right)\\ F(\sigma_{t+\Delta t}, \varepsilon^{p}_{nt}, \varepsilon^{p}_{t+\Delta t}, \sigma_{pt}, \lambda_{t+\Delta t}) = 0\end{gathered} \tag{S2}$$

- And a *pseudo-elastoplastic* increment (PEP), where σ, λ, ε^{p} and σ_{p} are updated.

$$\begin{gathered}\sigma_{t+\Delta t} = A_{t+\Delta t}\left(\varepsilon_{t+\Delta t} - \varepsilon^{p}_{t} - \Delta\lambda\left(\frac{\partial F}{\partial\sigma}\right)_{t+\Delta t}\right)\\ F(\sigma_{t+\Delta t}, \varepsilon^{p}_{nt}, \varepsilon^{p}_{t+\Delta t}, \sigma_{pt}, \lambda_{t+\Delta t}) = 0\\ G(\varepsilon^{p}_{nt}, \varepsilon^{p}_{t+\Delta t}, \sigma_{pt+\Delta t}, \lambda_{t+\Delta t}) = 0\end{gathered} \tag{S3}$$

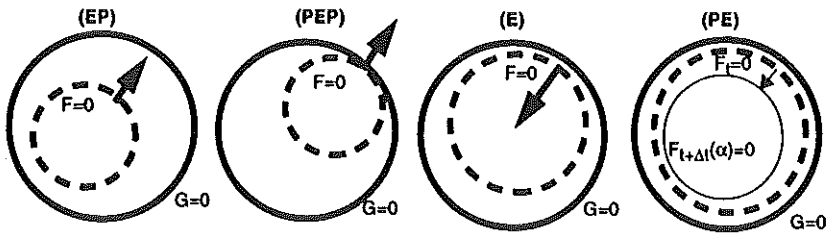

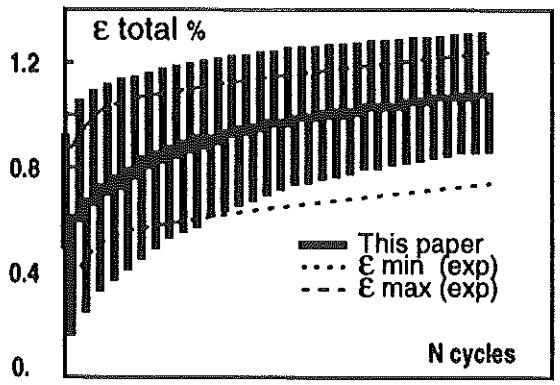

Fig 3a Uniaxial stress-controlled test used for identification (6).

The integration algorithm first makes an *elastic prediction*, in order to decide if the increment is (E)/(PE) or (EP/(PEP), and then makes a *plastic prediction* to choose between (EP) or (PEP) integration. The algorithm presented hereafter has been implemented in the *Code Aster*©, developed at Electricité de France (5). The three nonlinear implicit systems of tensorials equations (S1, S2, S3) are solved by a Newton method.

6 Comparison with Experiments

We use the following definitions for isotropic and kinematic hardenings

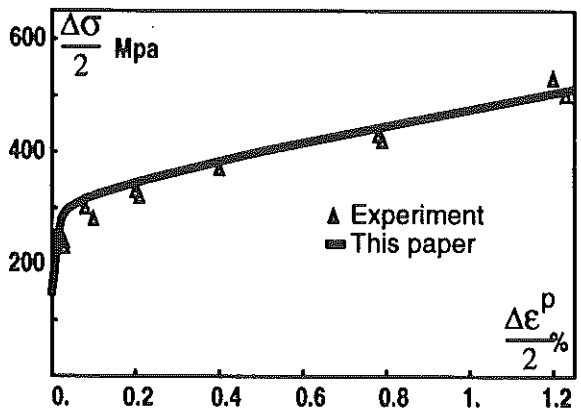

Fig 3b Cyclic stress–strain curve used for identification (12).

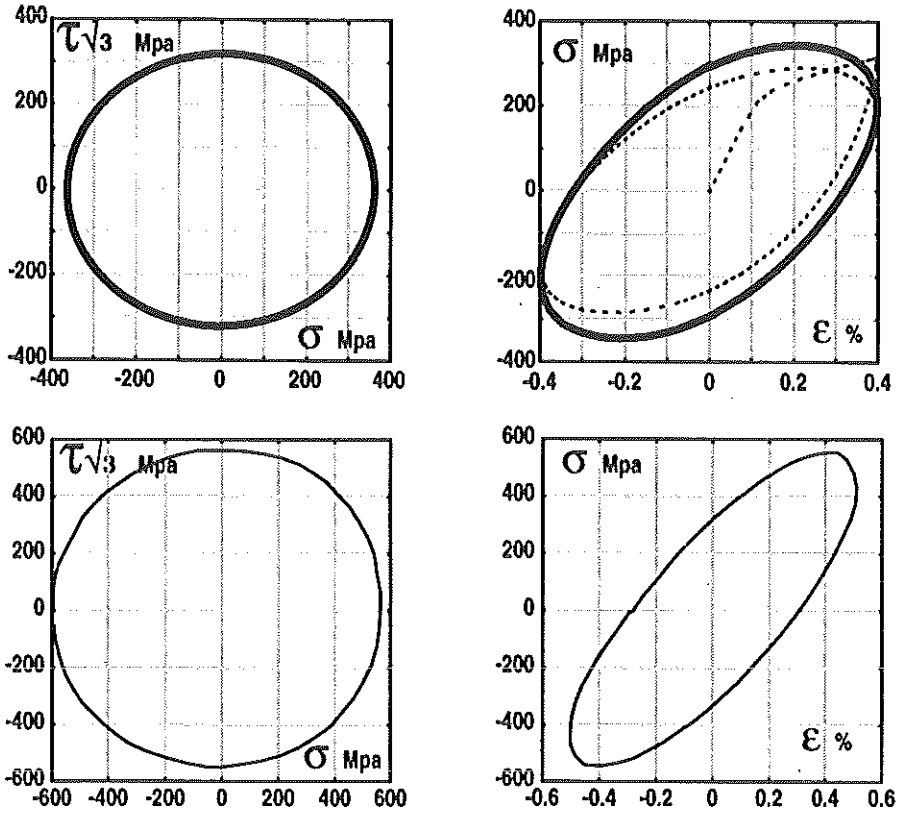

Fig 4 Circular loading. —— Steady-state simulation (this paper); — Steady-state experiment (10); ---- First cycle.

$$R = D(A|\varepsilon_p - \varepsilon_p^n|^\alpha + R_0) \qquad C = C_\infty + C_1 e^{-bl\left(1-\frac{\sigma_p}{S}\right)} \qquad D = 1 - me^{-bl\left(1-\frac{\sigma_p}{S}\right)}$$
$$X = C(s\varepsilon_p - \sigma_p\varepsilon_p^n)$$

The parameter identification is made using uniaxial curves taken from literature, then the comparison with nonproportional data is made with previous work. This is to test the robustness of the method. These results are presented in this paper.

The parameter identification is made also on uniaxial or nonproportional loadings. This is to test the precision of the method. The results are presented in (15).

6.1 *Identification in uniaxial case*

Uniaxial strain (12) and stress-controlled (6) tests have been used for the

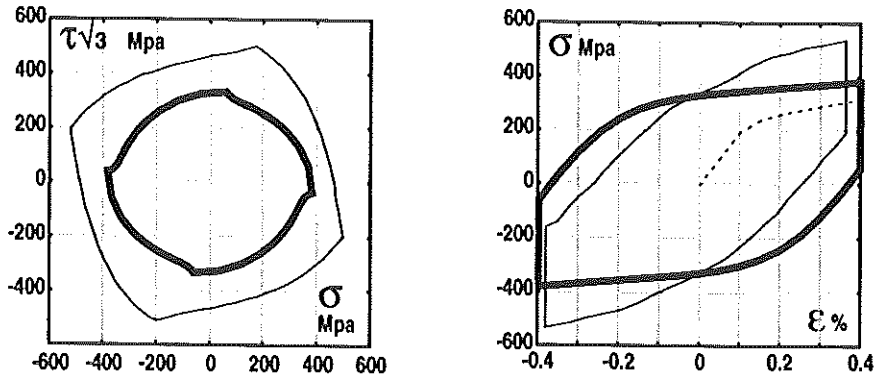

Fig 5 Square loading. —— Simulation (this paper) – Steady-state, only uniaxial identification used; ---- Simulation (this paper) – first cycle; — Experiment (10) – Steady-state.

identification, as shown in Fig. 3a and Fig. 3b. For parameter identification the software *Sidolo* is used (9).

$S = 800$ Mpa	$A = 341$ Mpa	$C = 5.8$	$R_0 = 150$ Mpa
$C_1 = 6.8$	$m = 0.264$	$\alpha = 0.122$	$b = 11$

6.2 *Simulation in multiaxial case*

Strain-controlled tension–torsion tests have been reported (**10**) on circular, square, one-step and two-step loading defined in the $(\varepsilon, \gamma/\sqrt{3})$ plane for a 316 stainless steel, at 20°C. Figures 4–7 show the results of simulations obtained by our model at steady states in the $(\sigma, \sqrt{3}\tau)$ plane and in the (σ, ε) plane for $\Delta\varepsilon_{eq} = 0.8\%$. We compare these results with experimental data given in (**10**). However, note that the data concerning circular loading is obtained for

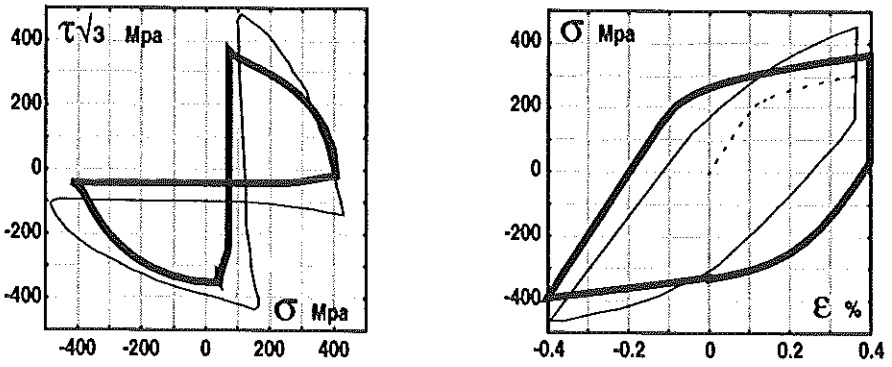

Fig 6 One-step loading. —— Simulation (this paper) – Steady-state, only uniaxial identification used; ---- Simulation (this paper) – first cycle; — Experiment (10) – Steady-state.

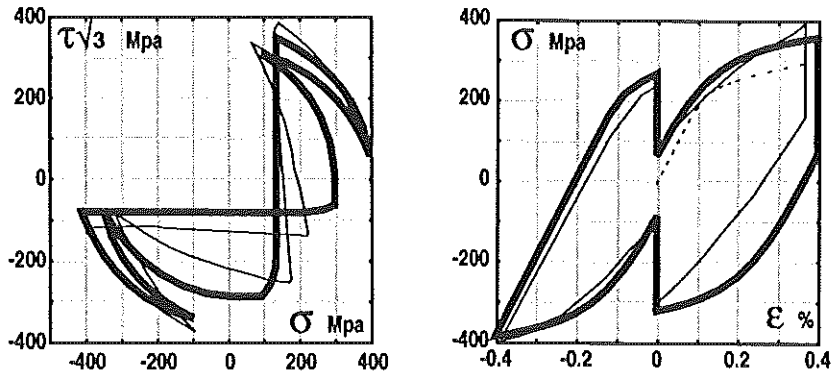

Fig 7 Two-step loading. —— Simulation (this paper) – Steady-state, only uniaxial identification used; ---- Simulation (this paper) – first cycle; — Experiment (10) – Steady-state.

$\Delta\varepsilon_{eq} = 1\,\%$, so in this case, the simulations and experimental data have been reported on two differents figures, with differents scales.

Constant tension cyclic strain torsion tests for the study of ratchetting have already been reported (11). Figure 8 gives a comparison for axial ratchetting between our model and two other constitutive laws. The first one is a Chaboche model with two kinematical variables (12). The second one is a two kinematical Chaboche law modified by Burlet–Cailletaud with the introduction of a radial fading memory (13, 14). It is worth noting that for this second model, tension–torsion tests have been used for identifications.

7 Conclusion

A cyclic elastoplastic constitutive law is proposed. Only uniaxial identification is used. This model gives much better results for ratchetting compared to the classical Chaboche model. Compared to models identified on multiaxial data, using a nonproportional parameter which is not the case for the present model, acceptable results are obtained. However, for the case of square loading, we believe the over-hardening has not been taken sufficiently into account, even if the uniaxial data used for identification is not of the same sample as the multiaxial data.

References

(1) TAHERI, S. (1989) Une loi de comportement uniaxial cyclique avec variable à mémoire discrète, *9ème Congres Francais de Mècanique*, Metz. France.

(2) TAHERI, S. (1991) A uniaxial cyclic clasto-plastic constitutive law with a discrete memory variable, *SMIRT 10*, L22, Tokyo, Japan.

(3) ANDRIEUX, S. and TAHERI, S. (1992) A cyclic constitutive law for metal with a semi-discrete memory variable for description of ratchetting phenomena. Report E.D.F/D.E.R/HI–71/7814.

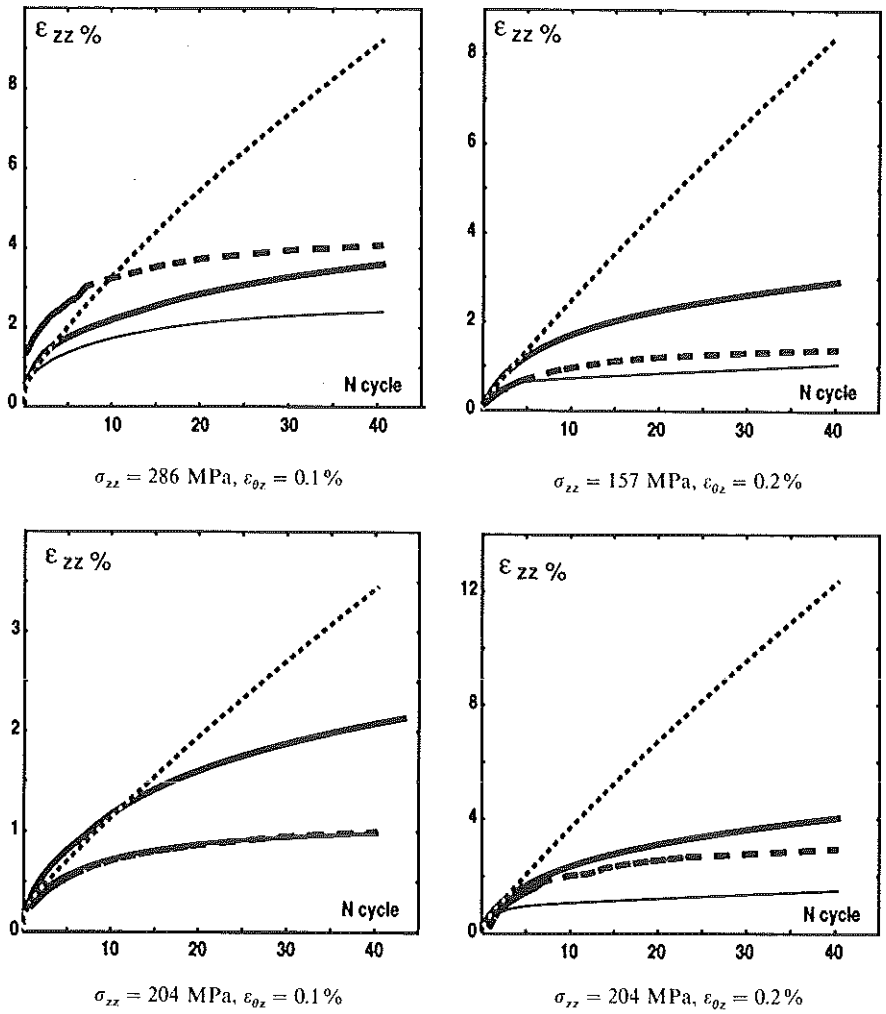

Fig 8 Constant tension cyclic torsion tests. —— This paper – only uniaxial identification used; ------ Chaboche – only uniaxial identification used; — Chaboche modified – nonproportional identification used; – – – – Experiment (11).

(4) *Code Aster* ©*v.2*, (1992) Analyse des Structures et Thermo-mécanique pour des Etudes et des Recherches. Manuel d'utilisation / Manuel descriptif Informatique / Manuel de reference, E.D.F/D.E.R.

(5) ANDRIEUX, S., SCHOENBERGER PH and TAHERI, S. (1993) A three-dimensional cyclic constitutive law for metal with a semi-discrete memory variable, *SMIRT 11*, L22, Stuttgart, Germany.

(6) PELLISSIER-TANON, A., BERNARD, J. L., AMZALLAG, C. and RABBE, P. (1980) Evaluation of the resistance of type 316 stainless steel against progressive deformation, *Int Sym. on Low-cycle Fatigue and Life Prediction*, Firminy, France.

(7) CHABOCHE, J. L. (1991) On some modifications of kinematical hardening to improve the description of ratcheting effect, *Int. J. of Plasticity*, **7**, pp. 661–678.
(8) GUIONNET, CH. (1989) Modélisation de la deformation progressive dans les essais biaxiaux, Rapport CEA – DEMT/89 – 120.
(9) GEYER, Ph., PROIX, J. M., SCHOENBERGER, Ph. and TAHERI, S. (1993) Modeling of ratcheting, Collection de notes internes, DER, 93NB00153.
(10) BENALLAL, A. and MARQUIS, D. Effects of nonproportional loadings in cyclic elastoviscoplasticity; Experimental theoretical and numerical aspects. *Engineering Computations*, **5**, (3), pp. 241–248.
(11) COUSSERAN, P., LEBEY, J., ROCHE, R. and CORBEL, P. (1980) Essais de déformation progressive de l'acier inoxydable 316L à la temperature ambiante, Rapport CEA-N-2139.
(12) ENGEL, J. J. and ROUSSELIER, G. (1985) Comportement en contrainte uniaxiale sous chargement cyclique de l'acier inoxydable austenitique 17-12 Mo à très bas carbone et azote controle, EDF/DER, rapport HT/PCD 599 MAT T 43.
(13) BURLET, H. and CAILLETAUD, G. (1987) Modelling of cyclic plasticity in finite element codes *2th Int. Conf. on Constitutive Laws for Engineering Materials, Theory and Application*, Tucson, Arizona.
(14) GEYER, PH. (1993) Modélisation des phénomènes de deformation progressive par le modèle elastoplastique de Chaboche modifié par Burlet et Cailletaud. EDF/DER, rapport HT26/93/052A.
(15) GEYER, Ph., JAYET-GENDROT, S., PROIX, J. M. and TAHERI, S. (1995) Three-dimensional elastic-plastic constitutive law for the description of ratchetting of 316 stainless steel, *SMIRT 95*.